GEOLOGY | THE GEOLOGICAL SOCIETY OF AMERICA®

https://doi.org/10.1130/G53764.1

Manuscript received 23 July 2025
Revised manuscript received 14 October 2025
Manuscript accepted 15 November 2025

Published online 2 December 2025

Mantle-driven, climatically modulated landscape evolution in Southern Patagonia

Victoria M. Fernandes[1,2,*], Andreas Ruby[1], Fergus McNab[1], Hella Wittmann[1], Andrew D. Wickert[1,3], Lennart Grimm[1], and Taylor Schildgen[1,4]

[1]GFZ Helmholtz Centre for Geosciences, 14473 Potsdam, Germany
[2]School of Earth, Atmosphere and Environment, Monash University, 9 Rainforest Walk, Clayton, 3800 Victoria, Australia
[3]St. Anthony Falls Laboratory and Department of Earth & Environmental Sciences, University of Minnesota, Minneapolis, Minnesota 55455, USA
[4]Institute for Geosciences, University of Potsdam, 14476 Potsdam, Germany

ABSTRACT

We explore the relative importance of tectonic, geodynamic, and surface processes in driving landscape evolution in Argentine Patagonia using 64 new ^{10}Be exposure ages of fluvial terraces preserved over >250 km along the Shehuén and Santa Cruz rivers (50°S). Terrace ages range from 33 ka to 1.5 Ma and coincide with Patagonian glaciations. We demonstrate that landscapes can respond directly to changes in climate forcing driven by the Mid-Pleistocene Transition: our results reveal a transition to 100-k.y. terrace periodicity, and a transient phase of accelerated incision starting at ca. 1 Ma. A regionally uniform incision rate of 130–180 m Ma^{-1} since 1 Ma suggests uplift linked to asthenospheric heating in the Patagonian slab window, while transient accelerated incision suggests convective instabilities in a low-viscosity mantle. We establish a temporal link between climate oscillations, fluvial incision, and mantle-driven epeirogenic uplift.

INTRODUCTION

Landscapes are the product of complex interactions between climate, tectonic, and surface processes operating over multiple spatial and temporal scales. Disentangling their relative contributions is challenging; tectonic and climatic signals tend to mask one another, and isolating long-term geodynamic drivers requires data that span sufficiently long spatial and temporal scales.

The Southern Patagonian steppe uniquely combines an absence of crustal deformation (Lagabrielle et al. 2004), pronounced geodynamic influences (Dávila and Lithgow-Bertelloni, 2013), and prominent glaciation (Mercer, 1983), which occur within the semi-arid rain shadow of the Andes (~300 mm a^{-1}; Blisniuk et al., 2005). This setting creates an ideal framework for isolating geomorphic responses to climate and geodynamics, where geomorphic features are preserved without the confounding overprint of orogenic activity.

Since 14 Ma, the subducting Chile Triple Junction has migrated north from 54°S to 46°S, progressively opening a slab window beneath South America (Fig. 1A; Lagabrielle et al., 2004), influencing regional magmatism, uplift, and landscape evolution (Gorring et al., 1997; Guillaume et al., 2009; Tobal et al., 2021). East of the thrust front, the foreland has been tectonically quiescent since the late Miocene (Lagabrielle et al., 2004). Epeirogenic uplift along the Patagonian coastline has been attributed to dynamic topography (Guillaume et al., 2009; Dávila and Lithgow-Bertelloni, 2013; Hollyday et al., 2023) or an isostatic response to lithospheric thinning (Ávila and Dávila, 2020), consistent with observed thin lithosphere, hot asthenosphere, and low mantle viscosity (Mark et al., 2022).

The record of epeirogenic uplift in Patagonia is not temporally continuous. Coastal outcrops of intertidal deposits constrain paleo–sea level and vertical motions since the early Pliocene (4.69–5.23 Ma; Hollyday et al., 2023), while marine terraces record uplift from Marine Isotope Stage (MIS) 11 (424 ka; Pedoja et al., 2011) to the late Holocene (3000 yr B.P.; Rubio-Sandoval et al., 2024). The morphology of fluvial terraces in Patagonia has been used to infer regional-scale mantle-driven uplift and foreland surface tilting, but its timing is poorly resolved (Guillaume et al., 2009; Tobal et al., 2021). Records of vertical motions of the Patagonian steppe that span this temporal gap and extend inland are thus critical for understanding the evolution of the slab window and the landscape above it.

Glacial activity, comprising waxing and waning of the Patagonian ice sheet in response to orbitally driven climate cycles, is also an important driver of landscape change in the region (Schellmann, 2000). Shorter mantle relaxation times due to low-viscosity mantle within the slab window enhance glacio-isostatic responses to ice-volume fluctuations (Dietrich et al., 2010). Regional glacial chronologies (Mercer, 1983; Ton-That et al., 1999; Rabassa et al., 2005; Clague et al., 2020; Hein et al., 2011; Tobal et al., 2021; see Supplemental Material[1]) form a near-continuous record since ca. 7 Ma. Critically, this record spans the Mid-Pleistocene Transition (MPT, 1.2–0.8 Ma), a time when a shift in the dominant periodicity of Earth's cli-

*milanez@gfz.de

[1]Supplemental Material. Text: 1. Field photographs (10). 2. References for mapping moraines, basalt flows and fluvial terraces. 3. Extraction of terrace paleo-profiles. 4. Depth profile modeling methods and parameters. 5. Terrace sample collection and exposure age calculation (CREp). 6. Terrace age interpretation. 7. Patagonian glacial chronology and correlation with terrace ages. 8. Uplift calculations for heated asthenosphere. Supplemental Dataset 1: Sample information and data for reproducing ^{10}Be exposure ages. Supplemental Dataset 2: Terrace longitudinal profile data (Figs. 1C and 1D). Please visit https://doi.org/10.1130/GEOL.S.30651332 to access the supplemental material; contact editing@geosociety.org with any questions.

CITATION: Fernandes, V.M., et al., 2026, Mantle-driven, climatically modulated landscape evolution in Southern Patagonia: Geology, v. 54, p. 117–122, https://doi.org/10.1130/G53764.1

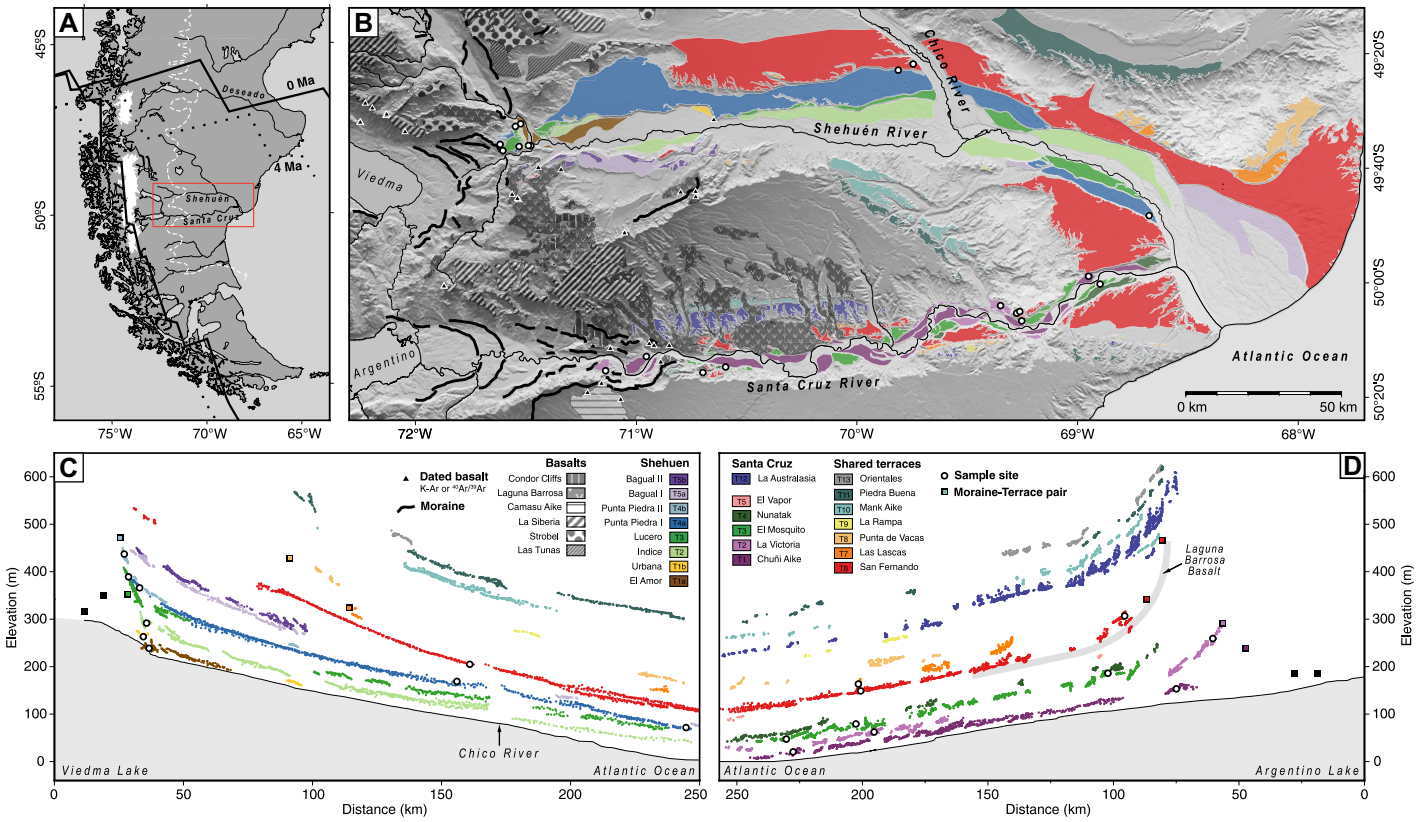

Figure 1. (A) Regional map showing evolution of the slab window (solid and dotted black lines), maximum extent of Patagonian ice during the Great Patagonian Glaciation (white dashed line), and study area (red box). (B) Santa Cruz and Shehuén Rivers, mapped terraces, basalt flows, and moraines. (C) Paleo-profiles of the Shehuén and (D) Santa Cruz terraces.

mate significantly impacted landscape evolution, particularly in regions sensitive to glacial dynamics (Valla et al., 2011).

Enhanced river incision associated with this climatic shift has been recognized in the Central Andes (Pingel et al., 2019) and Patagonia (Lagabrielle et al. 2007; Tobal et al., 2021). While 100-k.y. cyclicity of fluvial terrace abandonment has been observed in Andean rivers (Orr et al., 2024), sparse absolute chronologies of Patagonian terraces have led to only speculation on the role of the MPT in enhancing fluvial and glacial incision (Tobal et al., 2021) and preclude assessment of the relative contributions of climate and geodynamics on landscape evolution.

By mapping and dating fluvial terraces along the Santa Cruz and Shehuén rivers (50°S), we establish a detailed Pleistocene history of river incision. We then explore the extent to which regional climate versus deep-Earth processes may have contributed to river incision.

STUDY AREA

Fluvial terraces extend >250 km along the Santa Cruz and Shehuén rivers (Fig. 1B). Water and sediment are supplied by the San Martín, Viedma, and Argentino lakes (49–50°S), which in turn are fed by meltwater from the Southern Patagonian Icefield. Fill terraces comprise coarse gravel and cobbles in a sandy matrix, occasionally overlying outcrops of marine-derived Oligo-Miocene bedrock (see Supplemental Material).

Upstream, several terraces coincide with terminal moraines, pointing to a glacial origin (see Supplemental Material). The oldest cosmogenic ^{10}Be dated moraines in the Argentino–Viedma–San Martín valleys are 245 ka (Romero et al., 2024), although older moraine sequences are mapped (Schellmann, 2000). Local interbedded till and dated basalt flows constrain early Pleistocene glaciations to 1.08 Ma and older (Singer et al., 2004).

In the Santa Cruz valley, stacked basalt flows at Condor Cliffs (50.2°S, 70.9°W) range from 3.25 ± 0.08 Ma at the base (Clague et al., 2020) to 1.7 ± 0.5 Ma at the top (Schellmann, 2000). In the upper Shehuén valley, basalt flows are dated between 3.1 ± 0.15 Ma and 2.13 ± 0.09 Ma (Wenzens, 2000; Clague et al., 2020). In both valleys, these flows are, in places, overlain and underlain by till or preserve remnant terrace fill above them. The ages and distribution of basalt flows show that the paleo–Santa Cruz River flowed in a valley floor 100 m above its present level between 3.2 Ma and 1.7 Ma. The valley subsequently experienced multiple cycles of fill and incision, producing the terraces observed today.

METHODS

We mapped basalt flows using geological maps, satellite imagery, and field observations. Locations of moraine deposits were compiled from existing geomorphic maps and additional field mapping. We mapped fluvial terraces using TanDEM-X (12-m resolution) digital elevation data, complemented by 1:250,000 scale geological maps and other works, and correlated terrace patches based on elevation and stratigraphic relationships with basalt flows (see Supplemental Material). Terrace paleo-profiles were generated by projecting elevations for each terrace level to a valley center-line (see Supplemental Material for details).

To determine terrace abandonment ages, we measured in situ produced cosmogenic ^{10}Be from 53 cobble and 11 amalgamated pebble samples (N = 100 for each sample, 1–3 cm diameter) from terrace surfaces. To minimize the influence of erosion or burial on exposure ages, sample locations were chosen tens of meters from the closest terrace edge, gully, or alluvial fan. All cobbles collected were smooth and well rounded, suggesting minimal post-transport erosion of the cobble itself. Patches of surface loess raise the possibility of intermittent burial/erosion. We also collected a 4-sample depth profile from the lowest terrace

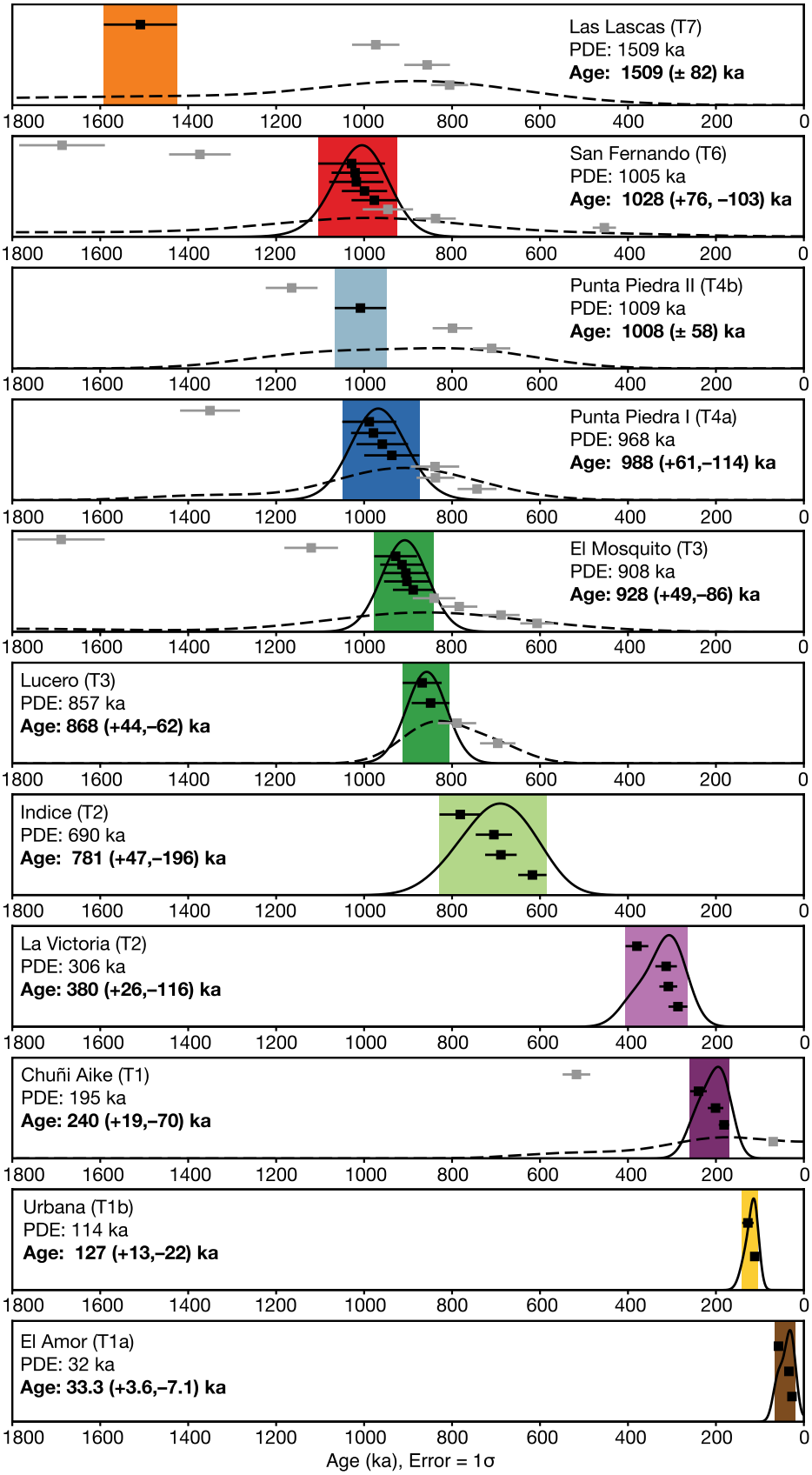

Figure 2. Terrace ages. Black squares—analyzed ages; gray squares—outlier ages; dashed line—probability density estimate (PDE) including all samples for terrace; solid line—PDE without outliers.

of the Shehuén River, comprising amalgamated pebble samples (N >100, 1–3 cm diameter) from the surface to 1.5 m depth, with each sample collected within a 10 cm depth interval. Details of sampling locations, preparation, analysis, exposure-age calculation, and age interpretation are provided in the Supplemental Material.

RESULTS

We identify six unique terrace levels in the Santa Cruz valley, eight in the Shehuén, and seven shared by both valleys. The San Fernando terrace (Figs. 1 and 2) is continuous along both rivers, providing a regional stratigraphic marker. Field observations confirm that the San Fernando terrace stratigraphically overlies the youngest basalt at Condor Cliffs, constraining its age to $<1.7 \pm 0.5$ Ma (Strelin and Malagnino, 2009; Clague et al., 2020; Supplemental Material). In their downstream reaches (>100 km), terraces are sub-parallel, with slopes similar to the modern floodplain (Figs. 1C and 1D).

Depth profile modeling (Fig. 3A and 3B) of the youngest terrace in the Shehuén valley yields an exposure age of $33.3^{+3.6}_{-7.1}$ ka and an inherited ^{10}Be concentration of $6.4^{+2.1}_{-3.9} \times 10^4$ at g^{-1}. Individual cobble and amalgamated pebble exposure ages from each terrace level were combined to determine the age of five terrace levels in the Santa Cruz and seven in the Shehuén valley (Fig. 2). Terrace ages range from 33 ka to 1.5 Ma. Ages grouped by terrace level form statistically coherent and stratigraphically consistent age populations (i.e., increase with elevation), especially when outliers are removed (see Supplemental Material). We interpret old and young outliers to reflect anomalous inheritance and erosion, respectively (cf. Hein et al., 2011; Tobal et al., 2021). The Las Lascas terrace age is poorly constrained but is at most 1510^{+82}_{-82} ka. The San Fernando terrace has an age of 1028^{+76}_{-103} ka, with subsequent terraces formed within 100 k.y. (Punta Piedra II = 1008^{+58}_{-58} ka, Punta Piedra I = 988^{+61}_{-114} ka). Lower terraces form in ~100 k.y. intervals (El Mosquito = 928^{+49}_{-86} ka, Lucero = 868^{+44}_{-62} ka, Indice = 781^{+47}_{-196} ka), with a 400 k.y. gap to the following levels, which also form in ~100 k.y. intervals (La Victoria = 380^{+26}_{-118} ka, Chuñi Aike = 240^{+19}_{-70} ka, Urbana = 127^{+13}_{-22} ka, El Amor = $33.3^{+3.6}_{-7.1}$ ka).

Our terrace mapping (see Supplemental Material) and interpreted ages reveal a similar timing and pattern of incision along the Shehuén and Santa Cruz valleys (Figs. 3C and 3D). At ca. 1 Ma, both valleys experienced rapid incision (660–2250 m Ma^{-1}), with a subsequent reduction for the Shehuén to 293 m Ma^{-1} between ~1000 ka and 800 ka. Starting at ~900–800 ka, incision rates dropped substantially (24–49 m Ma^{-1}), then increased again after 400 ka (88–181 m Ma^{-1}).

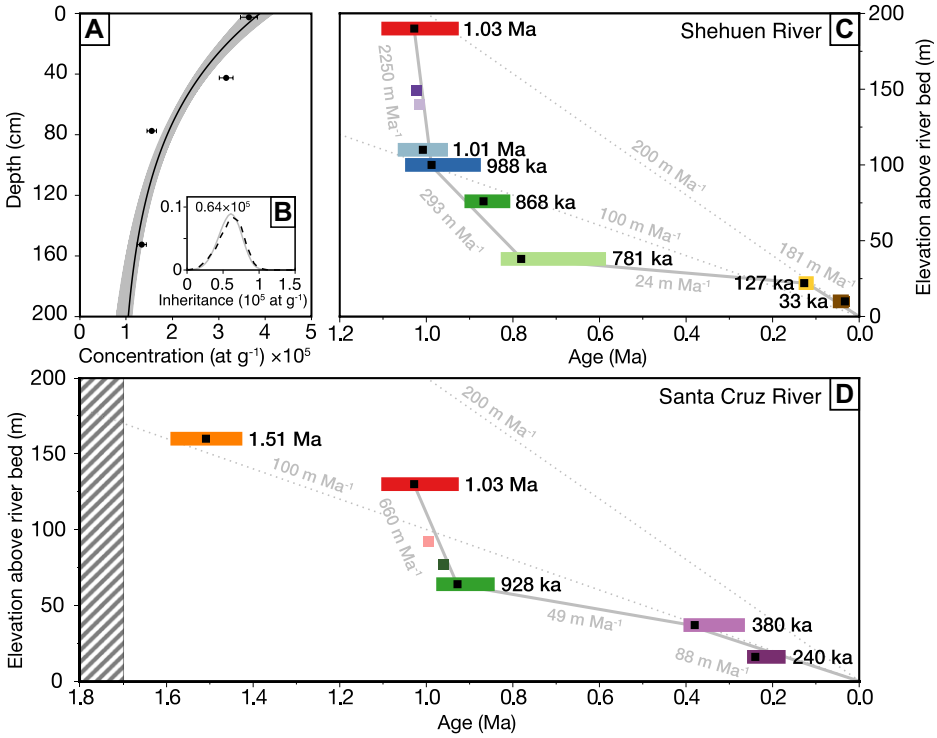

Figure 3. (A) Modeled depth profile and (B) inheritance. (C) Age-elevation plot of Shehuén and (D) Santa Cruz terraces. Dotted lines—uplift rates from Pedoja et al. (2011); solid gray lines—calculated incision rates (this study); black squares—interpreted terrace ages; colored bars—age range (Fig. 2). Empty colored squares represent undated terrace levels. Stippled area—dated basalts (Clague et al., 2020).

DISCUSSION AND CONCLUSIONS

Climate Modulation of Incision

We interpret that the San Fernando (1028 ka), Punta Piedra II (1008 ka), and Punta Piedra I (988 ka) terrace levels formed in response to multiple glaciations associated with the Great Patagonian Glaciation (GPG, Fig. 4; Mercer, 1983; Griffing et al., 2022). Additional undated terrace levels that lie between these must have formed between 1028 ka and 1008 ka in the Shehuén valley (Bagual I and II; Fig. 3C) and between 1028 ka and 928 ka in the Santa Cruz valley (Fig. 3D).

Post-GPG terraces can be correlated with major Patagonian glaciations during global glacial periods (MIS 24, 22, 20, 10, 8, 6, and 3; Fig. 4; see Supplemental Material). The terrace chronology spans the MPT and shows a transition from shorter periodicity (1028, 1008, 988 ka) to ~100-kyr periodicity (928, 868, 781, 380, 240, 127, 33 ka), suggesting that the landscape is responding to cyclic climate forcing, likely through variations in the sediment-to-water discharge ratio (McNab et al., 2023).

Accelerated incision at ca. 1 Ma, as observed in this study, has also been observed in glacial landscapes of Southern Patagonia (Torres del Paine, 51°S; Muller et al., 2024a). A change in precipitation across the foreland cannot explain the accelerated incision due to low rainfall since the Miocene (Blisniuk et al., 2005). Greater ice accumulation during the GPG, coinciding with the MPT, may have enhanced glacial erosion, and increased meltwater discharge during post-GPG deglaciations may have incised fluvial valleys downstream (Kaplan et al., 2009; Clague et al., 2020).

The observed temporal gap in the terrace record must be an artifact of preservation, since a quasi-continuous record of glaciations exists for MIS 20–10 in Northern Patagonia (Fig. 4). Preservation of terrace sequences requires net incision. Since downstream terrace slopes are sub-parallel to the current channel, and the incision history of the Santa Cruz and Shehuén rivers is similar to that of the Deseado River, 47°S (Tobal et al., 2021), it is likely that external factors modulating incision rate control terrace preservation.

Glacio-isostatic adjustment in response to variable glacial loading from the Patagonian ice sheet offers a plausible mechanism that modulates incision on such scales. Uplift of a peripheral bulge can significantly alter fluvial incision (e.g., Pico et al., 2019). However, the

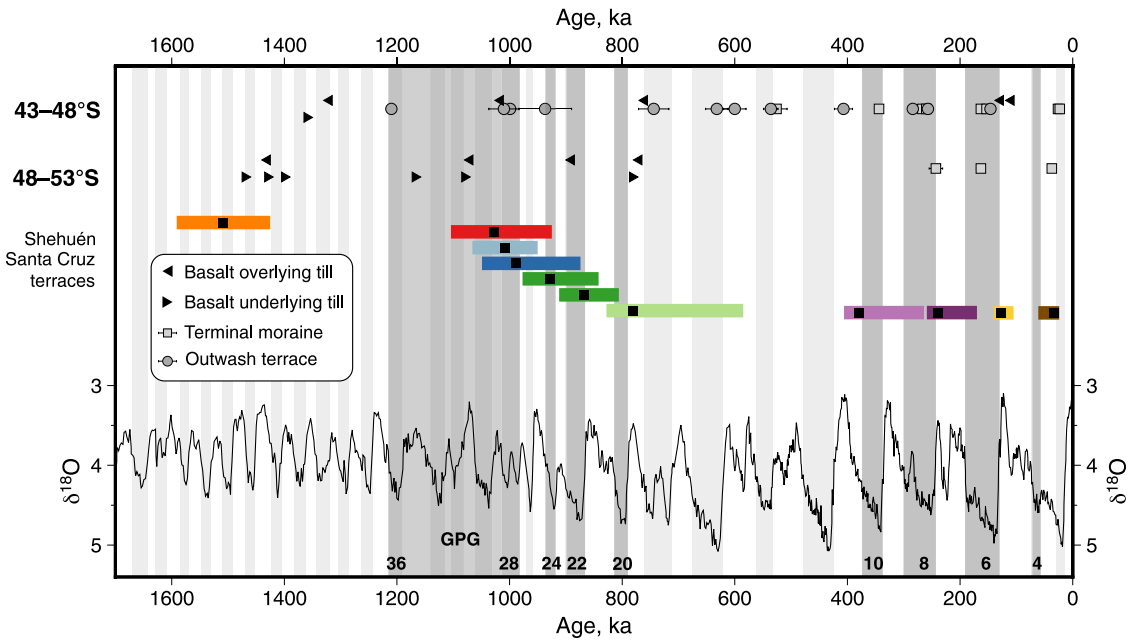

Figure 4. Patagonian glaciations and terrace ages. Top: Age constraints of glaciations in Northern (43–48°S) and Southern (48–53°S) Patagonia (see Supplemental Material for references; see text footnote 1). Colored bars with black squares—interpreted terrace ages (Fig. 2). Bottom: $\delta^{18}O$ record from Lisiecki and Raymo (2005). Numbers identify Marine Isotope Stage glaciations associated with terrace formation.

low elastic thickness of the Patagonian lithosphere limits terrace formation by this mechanism to <200 km from the main ice load (Dietrich et al., 2010), which may only explain steepened slopes at the upstream ends of the terraces (<50 km; Figs. 1C and 1D). Glacio-isostatic adjustment models suggest a maximum surface tilting of ~18 m across the entire river system over the past 5 m.y. (Hollyday et al., 2023), which is insufficient to explain the incision-rate variations.

Mantle Drivers of Landscape Evolution

Fluvial incision rates derived from post–MIS 11 terraces of the Shehuén and Santa Cruz rivers (181–88 m Ma^{-1}) are indistinguishable from long-term rates (184–106 m Ma^{-1} since ca. 1 Ma). Our terrace-derived incision rates are similar to other regional estimates (Figs. 3B and 3C): 138 m Ma^{-1} from 1.19 Ma incised basalt flows at Meseta Lago Buenos Aires (Lagabrielle et al. 2007), 135 m Ma^{-1} from ^{10}Be dated terraces of the Deseado River, 46.5°S (Tobal et al., 2021), and purported 100–200 m Ma^{-1} regional (42–55°S) coastal uplift rates since MIS 11 (Pedoja et al., 2011), although age estimates from these coastal deposits are speculative. The uniformity in uplift and incision rates from the proglacial lakes to the Atlantic Ocean (>300 km), spanning 9° of latitude (~1000 km), supports earlier inferences that regional uplift and incision are responses to mantle convection.

Geodynamic models of residual topography in the Patagonian foreland suggest that lithospheric thinning has influenced long-term uplift, but only in the proximal foreland (Ávila and Dávila, 2020). Thermo-mechanical modeling of satellite-derived uplift rates suggests excess asthenospheric temperatures of 100–200°C in the slab window (Muller et al., 2024b), which could also generate regional uplift. If this excess temperature is regionally distributed, it could generate up to 1.4 km of isostatic uplift (see Supplemental Material). If emplacement of hot, buoyant mantle material occurred over time scales of slab window opening (ca. 10 Ma), uplift rates would be similar to our observed long-term incision rates (~140 m Ma^{-1}). While these mechanisms can explain long-term incision of the Santa Cruz and Shehuén rivers, they cannot explain the sub-million-year incision rate variations.

We suggest that both mean incision rates and transient incision accelerations reflect dynamic uplift resulting from convection in a low-viscosity mantle. Dynamic uplift is often modeled on time scales of 5–10 m.y., so that only vertical motions on length-scales $>10^3$ km are resolved. For example, predictions from mantle convection models suggest ~5 m of uplift across Southern Patagonia over the past 5–10 m.y. (Rovere et al., 2020), two orders of magnitude lower than our observed long-term incision rates. Finer resolution models suggest that small-scale dynamic uplift (~500 km wavelength) can vary on time scales of 1–10 m.y., and that convective instabilities can create static waves of dynamic topography of the order 10^2 m (Arnould et al., 2018). Since low mantle viscosity promotes small-scale convection, with mantle viscosities as low as 10^{18} Pa s within the slab window (Mark et al. 2022), it is possible that the short-term variations in incision rate reflect mantle convection instabilities on a sub-million-year time scale.

In summary, our fluvial terrace chronology reveals a glacial cycle transition into 100-k.y. periodicity, and an accelerated phase of incision since the onset of the MPT and the demise of the GPG. Regional patterns of mantle-driven uplift previously observed along the Patagonian coast extend inland, preserving terraces. Sub-million-year variations in incision rate may record convective instabilities in hot, low-viscosity asthenospheric mantle within the slab window.

ACKNOWLEDGMENTS

This work was supported by ERC (European Research Council) Consolidator Grant 863490 GyroSCoPe awarded to Schildgen and an Alexander von Humboldt Foundation research Fellowship to Wickert.

REFERENCES CITED

Arnould, M., Coltice, N., Flament, N., Seigneur, V., and Müller, R.D., 2018, On the scales of dynamic topography in whole-mantle convection models: Geochemistry, Geophysics, Geosystems, v. 19, p. 3140–3163, https://doi.org/10.1029/2018GC007516.

Ávila, P., and Dávila, F.M., 2020, Lithospheric thinning and dynamic uplift effects during slab window formation, southern Patagonia (45°–55° S): Journal of Geodynamics, v. 133, https://doi.org/10.1016/j.jog.2019.101689.

Blisniuk, P.M., Stern, L.A., Chamberlain, C.P., Idleman, B., and Zeitler, P.K., 2005, Climatic and ecologic changes during Miocene surface uplift in the Southern Patagonian Andes: Earth and Planetary Science Letters, v. 230, p. 125–142, https://doi.org/10.1016/j.epsl.2004.11.015.

Clague, J.J., Barendregt, R.W., Menounos, B., Roberts, N.J., Rabassa, J., Martinez, O., Ercolano, B., Corbella, H., and Hemming, S.R., 2020, Pliocene and Early Pleistocene glaciation and landscape evolution on the Patagonian Steppe, Santa Cruz province, Argentina: Quaternary Science Reviews, v. 227, https://doi.org/10.1016/j.quascirev.2019.105992.

Dávila, F.M., and Lithgow-Bertelloni, C., 2013, Dynamic topography in South America: Journal of South American Earth Sciences, v. 43, p. 127–144, https://doi.org/10.1016/j.jsames.2012.12.002.

Dietrich, R., Ivins, E.R., Casassa, G., Lange, H., Wendt, J., and Fritsche, M., 2010, Rapid crustal uplift in Patagonia due to enhanced ice loss: Earth and Planetary Science Letters, v. 289, p. 22–29, https://doi.org/10.1016/j.epsl.2009.10.021.

Gorring, M.L., Kay, S.M., Zeitler, P.K., Ramos, V.A., Rubiolo, D., Fernandez, M.I., and Panza, J.L., 1997, Neogene Patagonian plateau lavas: Continental magmas associated with ridge collision at the Chile Triple Junction: Tectonics, v. 16, p. 1–17, https://doi.org/10.1029/96TC03368.

Guillaume, B., Martinod, J., Husson, L., Roddaz, M., and Riquelme, R., 2009, Neogene uplift of central eastern Patagonia: Dynamic response to active spreading ridge subduction?: Tectonics, v. 28, TC2009, https://doi.org/10.1029/2008TC002324.

Griffing, C.Y., Clague, J.J., Barendregt, R.W., Ercolano, B., Corbella, H., Rabassa, J., and Roberts, N.J., 2022, Early and Middle Pleistocene glaciation of the southern Patagonian plain: Journal of South American Earth Sciences, v. 114, https://doi.org/10.1016/j.jsames.2021.103687.

Hein, A.S., Dunai, T.J., Hulton, N.R.J., and Xu, S., 2011, Exposure dating outwash gravels to determine the age of the greatest Patagonian glaciations: Geology, v. 39, p. 103–106, https://doi.org/10.1130/G31215.1.

Hollyday, A., Austermann, J., Lloyd, A., Hoggard, M., Richards, F., and Rovere, A., 2023, A revised estimate of early Pliocene global mean sea level using geodynamic models of the Patagonian slab window: Geochemistry, Geophysics, Geosystems, v. 24, https://doi.org/10.1029/2022GC010648.

Kaplan, M.R., Hein, A.S., Hubbard, A., and Lax, S.M., 2009, Can glacial erosion limit the extent of glaciation?: Geomorphology, v. 103, p. 172–179, https://doi.org/10.1016/j.geomorph.2008.04.020.

Lagabrielle, Y., Suárez, M., Rossello, E.A., Hérail, G., Martinod, J., Régnier, M., and de la Cruz, R., 2004, Neogene to Quaternary tectonic evolution of the Patagonian Andes at the latitude of the Chile Triple Junction: Tectonophysics, v. 385, p. 211–241, https://doi.org/10.1016/j.tecto.2004.04.023.

Lagabrielle, Y., et al., 2007, Pliocene extensional tectonics in the Eastern Central Patagonian Cordillera: Geochronological constraints and new field evidence: Terra Nova, v. 19, p. 413–424, https://doi.org/10.1111/j.1365-3121.2007.00766.x.

Lisiecki, L.E., and Raymo, M.E., 2005, A Pliocene-Pleistocene stack of 57 globally distributed benthic $\delta^{18}O$ records: Paleoceanography, v. 20, PA1003, https://doi.org/10.1029/2004PA001071.

Mark, H.F., Wiens, D.A., Ivins, E.R., Richter, A., Mansour, W.B., Magnani, M.B., Marderwald, E., Adaros, R., and Barrientos, S., 2022, Lithospheric erosion in the Patagonian slab window, and implications for glacial isostasy: Geophysical Research Letters, v. 49, https://doi.org/10.1029/2021GL096863.

McNab, F., Schildgen, T., Turowski, J.M., and Wickert, A.D., 2023, Diverse responses of alluvial rivers to periodic environmental change: Geophysical Research Letters, v. 50, https://doi.org/10.1029/2023GL103075.

Mercer, J.H., 1983, Cenozoic glaciation in the Southern Hemisphere: Annual Review of Earth and Planetary Sciences, v. 11, p. 99–132, https://doi.org/10.1146/annurev.ea.11.050183.000531.

Muller, V.A.P., et al., 2024a, Geodynamic and climatic forcing on late-Cenozoic exhumation of the Southern Patagonian Andes (Fitz Roy and Torres del Paine massifs): Tectonics, v. 43, https://doi.org/10.1029/2023TC007914.

Muller, V.A., Sternai, P., and Sue, C., 2024b, Fast uplift in the southern Patagonian Andes due to long-and short-term deglaciation and the asthenospheric window underneath: Solid Earth, v. 15, p. 387–404, https://doi.org/10.5194/se-15-387-2024.

Orr, E.N., Schildgen, T.F., Tofelde, S., Wittmann, H., and Alonso, R.N., 2024, Landscape response to tectonic deformation and cyclic climate change since ca. 800 ka in the southern Central Andes: Earth Surface Dynamics, v. 12, p. 1391–1413, https://doi.org/10.5194/esurf-12-1391-2024.

Pedoja, K., Regard, V., Husson, L., Martinod, J., Guillaume, B., Fucks, E., Iglesias, M., and Weill,

P., 2011, Uplift of quaternary shorelines in eastern Patagonia: Darwin revisited: Geomorphology, v. 127, p. 121–142, https://doi.org/10.1016/j.geomorph.2010.08.003.

Pico, T., Mitrovica, J.X., Perron, J.T., Ferrier, K.L., and Braun, J., 2019, Influence of glacial isostatic adjustment on river evolution along the U.S. mid-Atlantic coast: Earth and Planetary Science Letters, v. 522, p. 176–185, https://doi.org/10.1016/j.epsl.2019.06.026.

Pingel, H., Alonso, R.N., Altenberger, U., Cottle, J., and Strecker, M.R., 2019, Miocene to Quaternary basin evolution at the southeastern Andean Plateau (Puna) margin (ca. 24°S lat, Northwestern Argentina): Basin Research, v. 31, p. 808–826, https://doi.org/10.1111/bre.12346.

Rabassa, J., Coronato, A.M., and Salemme, M., 2005, Chronology of the Late Cenozoic Patagonian glaciations and their correlation with biostratigraphic units of the Pampean region (Argentina): Journal of South American Earth Sciences, v. 20, p. 81–103, https://doi.org/10.1016/j.jsames.2005.07.004.

Romero, M., et al., 2024, Late Quaternary glacial maxima in southern Patagonia: Insights from the Lago Argentino glacier lobe: Climate of the Past, v. 20, p. 1861–1883, https://doi.org/10.5194/cp-20-1861-2024.

Rovere, A., Pappalardo, M., Richiano, S., Aguirre, M., Sandstrom, M.R., Hearty, P.J., Austermann, J., Castellanos, I., and Raymo, M.E., 2020, Higher than present global mean sea level recorded by an Early Pliocene intertidal unit in Patagonia (Argentina): Communications Earth & Environment, v. 1, 68, https://doi.org/10.1038/s43247-020-00067-6.

Rubio-Sandoval, K., Ryan, D.D., Richiano, S., Giachetti, L.M., Hollyday, A., Bright, J., Gowan, E.J., Pappalardo, M., Austermann, J., Kaufman, D.S., and Rovere, A., 2024, Quaternary and Pliocene sea-level changes at Camarones, central Patagonia, Argentina: Quaternary Science Reviews, v. 345, https://doi.org/10.1016/j.quascirev.2024.108999.

Schellmann, G., 2000, Landscape evolution and glacial history of Southern Patagonia, Argentina, since the late Miocene—Some general aspects: Zentralblatt für Geologie und Paläontologie: Teil 1, Allgemeine, angewandte, regionale und historische Geologie, p. 1013–1026, https://fis.uni-bamberg.de/handle/uniba/10481.

Singer, B.S., Ackert, R.P., and Guillou, H., 2004, $^{40}Ar/^{39}Ar$ and K-Ar chronology of Pleistocene glaciations in Patagonia: Geological Society of America Bulletin, v. 116, p. 434–450, https://doi.org/10.1130/B25177.1.

Strelin, J., and Malagnino, E., 2009, Charles Darwin and the oldest glacial events in Patagonia: The erratic blocks of the Río Santa Cruz Valley: Revista de la Asociación Geológica Argentina, v. 64, p. 101–108, https://revista.geologica.org.ar/raga/article/view/1334.

Tobal, J.E., Morabito, E.G., Terrizzano, C.M., Zech, R., Colavitto, B., Struck, J., Christl, M., and Ghiglione, M.C., 2021, Quaternary landscape evolution of Patagonia at the Chilean Triple Junction: Climate and tectonic forcings: Quaternary Science Reviews, v. 261, https://doi.org/10.1016/j.quascirev.2021.106960.

Ton-That, T., Singer, B., Mörner, N.A., and Rabassa, J., 1999, Datación de lavas basálticas por $^{40}Ar/^{39}Ar$ y geología glacial de la región del lago Buenos Aires, Provincia de Santa Cruz, Argentina: Revista de la Asociación Geológica Argentina, v. 54, no. 4, p. 333–352, https://revista.geologica.org.ar/raga/issue/view/28.

Valla, P., Shuster, D., and van der Beek, P., 2011, Significant increase in relief of the European Alps during mid-Pleistocene glaciations: Nature Geoscience, v. 4, p. 688–692, https://doi.org/10.1038/ngeo1242.

Wenzens, G., 2000, Pliocene piedmont glaciation in the Río Shehuen Valley, southeast Patagonia, Argentina: Arctic, Antarctic, and Alpine Research, v. 32, p. 46–54, https://doi.org/10.1080/15230430.2000.12003338.

Printed in the USA